



Histone deacetylase inhibitor ITF2357 (givinostat) reverts transformed phenotype and counteracts stemness in in vitro and in vivo models of human glioblastoma

Francesco Marampon¹ · Flavio Leoni² · Andrea Mancini³ · Ilaria Pietrantonì⁴ · Silvia Codenotti⁵ · Ferella Letizia^{3,6} · Francesca Megiorni⁷ · Giuliana Porro² · Elisabetta Galbiati² · Pietro Pozzi² · Paolo Mascagni² · Alfredo Budillon⁸ · Roberto Maggio⁴ · Vincenzo Tombolini¹ · Alessandro Fanzani⁵ · Giovanni Luca Gravina^{3,6} · Claudio Festuccia³

Received: 4 September 2018 / Accepted: 17 November 2018 / Published online: 24 November 2018
© Springer-Verlag GmbH Germany, part of Springer Nature 2018

Abstract

Purpose Aberrant expression and activity of histone deacetylases (HDACs) sustain glioblastoma (GBM) onset and progression, and, therefore, HDAC inhibitors (HDACi) represent a promising class of anti-tumor agents. Here, we analyzed the effects of ITF2357 (givinostat), a pan-HDACi, in GBM models for its anti-neoplastic potential.

Methods A set of GBM- and patient-derived GBM stem-cell lines was used and the ITF2357 effects on GBM oncophenotype were investigated in in vitro and in vivo xenograft models.

Results ITF2357 inhibited HDAC activity and affected GBM cellular fate in a dose-dependent manner by inducing G₁/S growth arrest (1–2.5 μM) or caspase-mediated cell death (≥ 2.5 μM). Chronic treatment with low doses (≤ 1 μM) induced autophagy-mediated cell death, neuronal-like phenotype, and the expression of differentiation markers, such as glial fibrillar actin protein (GFAP) and neuron-specific class III beta-tubulin (Tuj-1); this reduces neurosphere formation from patient-derived GBM stem cells. Autophagy inhibition counteracted the ITF2357-induced expression of differentiation markers in p53-expressing GBM cells. Finally, in in vivo experiments, ITF2357 efficiently passed the blood–brain barrier, so rapidly reaching high concentration in the brain tissues, and significantly affected U87MG and U251MG growth in orthotopic xenotransplanted mice.

Conclusions The present findings provide evidence of the key role played by HDACs in sustaining transformed and stem phenotype of GBM and strongly suggest that ITF2357 may have a clinical potential for the HDACi-based therapeutic strategies against GBM.

Keywords Glioblastoma · Cancer stem cells · HDACs · HDACs' inhibitor · Givinostat · ITF2357

Introduction

Glioblastoma (GB) accounts more than 60% of all primary brain tumors. Despite multimodality therapeutic approaches, consisting of surgical debulking followed by radiotherapy combined to temozolomide chemotherapy, the median

survival is 12–15 months and all new therapeutic strategies have failed to prolong survival (Johnson and O'Neill 2012). Several genetic and epigenetic alterations have been related to GBM onset, progression, and resistance to therapies, with increasing evidences focused on the role of aberrant histone acetylation in tumor etiopathogenesis (Nagarajan and Costello 2009). Histones, nuclear proteins that package and order the DNA into structural units called nucleosomes, modifying the condensed chromatin status, affect gene transcription (Chen et al. 2015). Histone acetyltransferases (HATs), by acetylating the histones at specific aminoacid positions, open the condensed chromatin structure, thus, promoting gene transcription, whilst histone deacetylases (HDACs), by deacetylating histone tails, promote opposite effects (Chen et al. 2015). Consistent with their importance

Francesco Marampon and Flavio Leoni have contributed equally.

Giovanni Luca Gravina and Claudio Festuccia have contributed equally.

✉ Claudio Festuccia
claudio.festuccia@univaq.it

Extended author information available on the last page of the article

in controlling gene transcription, these enzymes are tightly regulated in living cells, and their activity can be modulated by several signaling pathways through cell surface receptors (Legube and Trouche 2003). Most recently, β -arrestins, a family of adaptor proteins that regulate the signaling and trafficking of G protein-coupled receptors (Zhu et al. 2017), have been shown to modify HAT and HDAC activity (Kang et al. 2005; Rosanò et al. 2013) and, in this way, regulate cancer invasion and metastasis (Song et al. 2018). Aberrant expression and/or activity of HDACs have been linked to tumorigenesis through the transcriptional silencing of anti-oncogenes, which finely control cell proliferation, cell cycle, and survival pathways (Glozak and Seto 2008). Thus, HDACs are strategic therapeutic targets for cancer treatment, and they have inspired researchers to study and develop different class of HDAC inhibitors (HDACi) (Eck-schlager 2017; De Souza and Chatterji 2015). Increasing pre-clinical and clinical experiences encourage the use of HDACi in treating GBM (Bezecny 2014) and new and more potent small-molecule HDACi, able to modulate the biological function of HDACs, are continuously synthesized and tested. Accordingly with the literature, our recent evidences confirm the therapeutic strategic role of targeting HDACs (Festuccia et al. 2018; Sferra et al. 2017; Marampon et al. 2017). This study describes the anti-tumor effects of the HDACi ITF2357 (givinostat) (Leoni et al. 2005) on several in vitro and in vivo GBM models. Treatment of GBM cell lines with ITF2356 significantly inhibited tumor cell growth or induced apoptosis in a dose-dependent manner, while the daily treatment promoted apoptosis, autophagy, or neuronal differentiation of surviving cells, dependently from the concentration used. Finally, ITF2357 counteracted GBM stem-like cell population and GBM tumor growth in xenograft mouse models.

Materials and methods

Cell lines, cell culture, and treatments

Twelve glioblastoma cell lines, representing grade III and IV gliomas, with different expression of methyl-guanine-DNA methyl-transferase (MGMT), drug, and radiation sensitivity, were obtained from the American Type Culture Collection (Rockville, MD) and maintained as already described (Festuccia et al. 2018; Sferra et al. 2017; Marampon et al. 2017, 2014). Periodically, DNA profiling using the GenePrint10 System (Promega Corporation, Madison, WI) was carried out to authenticate cell cultures, comparing the DNA profile of our cell cultures with those found in GenBank. Patient-derived glioblastoma stem cells were kindly provided from J. Gregory Cairncross and Samuel Weiss at the Hotchkiss Brain Institute, Faculty of Medicine, University of Calgary,

Calgary, Alberta, Canada (Kelly et al. 2009) and cultured in DMEM/F12 media without serum supplemented with 20 ng/ml epidermal growth factor (Sigma-Aldrich), 20 ng/ml basic fibroblast growth factor (Sigma-Aldrich), B-27 supplement 1X (Gibco, Life Technologies), and antibiotics, as previously described (Cusulin et al. 2015). ITF2357 was provided by Italfarmaco, Cinisello Balsamo, MI, Italy, dissolved in DMSO, stored at 4 °C and added 24 h after plating at the different concentrations used in the experiments.

In vitro assay inhibition of HDAC activity

The values of IC₅₀ concentrations of the HDAC inhibitor was determined in cell extracts using the HDAC Fluorimetric Assay/Drug Discovery Kit, designed to measure HDAC activity (BML-AK-500, Biomol), following the manufacturer's instructions.

Immunoblotting

Western blotting was conducted as previously described (Marampon et al. 2016; Vulcano et al. 2006) with the following antibodies: anti-Cyclin-dependent kinase inhibitor 1 (p21^{Cip1/Waf1}) (C-19), anti-Cyclin-dependent kinase inhibitor 1B (p27^{KIP1}) (C-19), anti-Cyclin A (H-432), anti-Cyclin B1 (H-433), anti-Cyclin-dependent kinase 1/2 (CDK1/CDK2) (AN21.2), anti-Caspase 3 (H277), anti-Caspase 9 (1–2), anti-Caspase 8 (1.1.40), anti-bcl-2-like protein 4 (Bax) (6A7), anti-B-cell lymphoma 2 (Bcl2) (C-2), anti- β -tubulin (TU-20), anti-Glial fibrillary acidic protein (GFAP) (C19), anti-Oligodendrocyte Transcription Factor 1 (Olig1) (E12), anti-Beclin1 (E-8), anti-Autophagy protein 5 (ATG5) (C-1), anti-Autophagy protein 7 (ATG7) (H-300), anti- α -tubulin (TU-02), anti-acetyl-Histone H3 (Lys9/14), anti-Histone H3 (FL-136), anti-acetyl-Histone H4 (Lys5), and anti-Histone H4 (H-97) all from Santa Cruz Biotechnology, and anti-CD144 (ab97478), anti-microtubule-associated protein 1A/1B-light chain 3 (LC3, ab51520), and anti-CD133 (ab19898) from Abcam. Peroxidase-conjugate anti-mouse or anti-rabbit antibodies (Amersham GE Healthcare) were used for enhanced chemiluminescence detection.

Cell growth, apoptosis analysis, cell cycle distribution, and Fas/CD95 flow cytometry

Cell growth was performed as previously described by treating cells with ITF2357 24 h after plating; for the outgrowth assay, growth medium-containing ITF2357 was removed after the indicated time and replenished with growth medium without drugs. Growth inhibition was determined using the CellTiter 96 AQueous One Solution Cell Proliferation Assay according to the manufacturer's instructions (Promega, Inc.). The absorbance was measured at 490 nm on a microplate

reader. Apoptosis was assessed by TUNEL assay from Bio-compare, accordingly with the manufacturer's instructions. Flow cytometry was performed using Tali[®] Cell Cycle Kit (Life Technologies Italia, Monza, Italy); stained cells were then measured using FACS which can flow cytometry (Becton Dickinson, USA). Fas/CD95 flow cytometry was performed with FITC–anti-CD95 from Abcam (ab87023).

Measurement of ITF2357 ability to cross the blood–brain barrier (BBB) and induce brain tissue hyper-acetylation

Sprague–Dawley rats (male, 250–275 g, Charles River Italy) were treated with ITF2357 in 0.5% methyl-cellulose by gavage at 50 and 100 mg/kg. After 1, 3, and 6 h following drug administration, the animals (3 rats/time point) were anaesthetized and sacrificed to collect the brain and three rats were sacrificed before drug administration (pre-dose, time 0). Brains were immediately placed in ice and then homogenized with a potter for 5 min in ice. Tissue extracts were centrifuged (14,000 rpm, Eppendorf micro-centrifuge) at 4 °C and pellets were submitted to acidic extraction according (Yoshida et al. 1990). Briefly, the homogenate was extracted with ice-cold lysis buffer 10 mM Tris•HCl, pH 6.5, 50 mM sodium bisulfite, 1% Triton X-100, 10 mM MgCl₂, 8.6% sucrose, and complete protease inhibitor mixture (Roche Molecular Biochemicals) for 20 min at 4 °C, and, then, centrifuged (14,000 rpm, Eppendorf micro-centrifuge) at 4 °C. The pellet was repeatedly washed with lysis buffer until the supernatant was clear. The nuclear pellet was washed with nuclear wash buffer (10 mM Tris-HCl, 13 mM EDTA, pH 7.4) and suspended in 0.2 M HCl and 0.2 M H₂SO₄ in distilled water. Nuclei were extracted overnight at 4 °C and the residue was centrifuged (14,000 rpm, Eppendorf micro-centrifuge) at 4 °C for 10 min. The supernatant was suspended in 1 mL of ice-cold acetone, left overnight at –20 °C, and, then, centrifuged (14,000 rpm, Eppendorf micro-centrifuge) at 4 °C for 10 min. The sample was washed with ice-cold acetone, dried, and diluted in distilled water. The amount of histone H3 and acetylated-histone H3 was determined by densitometry analysis of western blots (20 µg/lane, 8–12% PAGE) using anti-H3 (FL-136) and anti-acetylated H3 (Lys9/14) antibodies, both from Santa Cruz Biotechnology.

Xenograft model

Male CD1 nude mice (Charles River, Milan, Italy) were maintained under the guidelines established by our Institution (University of L'Aquila, Medical School and Science and Technology School Board Regulations), complying with the Italian government regulation no. 116 January 27, 1992 for the use of laboratory animals. All mice received subcutaneous flank injections of 1×10^7 GBM cancer cells. Tumor

growth was assessed bi-weekly by measuring tumor diameters with a Vernier caliper (length \times width). Tumor weight was calculated according to the formula: TW (mg) = tumor volume (mm³) = $d^2 \times D/2$, where d and D represent the shortest and longest diameters, respectively. The effects of the drug treatments were examined as previously described. Animals were sacrificed by carbon dioxide inhalation and tumors were subsequently removed surgically. A part of the tumor was directly frozen in liquid nitrogen for protein analysis and the other part was fixed in paraformaldehyde overnight for immunohistochemical analyses, including endothelial (CD31 and vWF, Dako, Glostrup, Denmark) and proliferation (Ki67, Dako) markers. Time-to-Progression (TTP) was calculated from the start of treatments to the local disease progression. Local tumor progression according to SWOG criteria was defined as the increase $> 50\%$ of the product of longest diameter and greatest perpendicular diameter.

Statistics

Continuous variables were summarized as mean and standard deviation (SD) or as median and 95% CI for the median. For continuous variables not normally distributed, statistical comparisons between control and treated groups were established by carrying out the Kruskal–Wallis Tests. For continuous variables normally distributed, statistical comparisons between control and treated groups were established by carrying out the ANOVA test or by Student t test for unpaired data (for two comparisons).

Results

ITF2357 efficiently inhibits HDACs and induces GBM G₁/S growth arrest or apoptosis in a dose-dependent manner

The dose of ITF2357 able to induce 50% of HDAC activity inhibition (IC₅₀) was investigated on 12 GBM cell lines treated for 24 h with increasing doses of ITF2357 (0.1, 0.25, 0.5, 1, 2.5, and 5 µM). ITF2357 significantly inhibited HDAC activity with an IC₅₀ dose range that was between 0.2 ± 0.03 µM in U87MG and 0.65 ± 0.08 µM in U251MG GBM cell lines (Fig. 1a). High- (U87MG), medium-(T98G), and low-ITF2357 (U251MG) responsive cell lines were then used. Treatment of U87MG (Fig. 1b), T98G (Fig. 1c), and U251MG (Fig. 1d) cells with IC₅₀ dose of ITF2357 for prolonged times rapidly and persistently promoted Histone-H3 (H3^{AC}), -H4 (H4^{AC}) and α -tubulin (α -Tub^{AC}) acetylation status. Immunoblotting performed 24 h after treating cells confirmed the ability of ITF2357 to promote Histone-H3, Histone-H4, and α -tubulin acetylation (Fig. 1e). The dose of

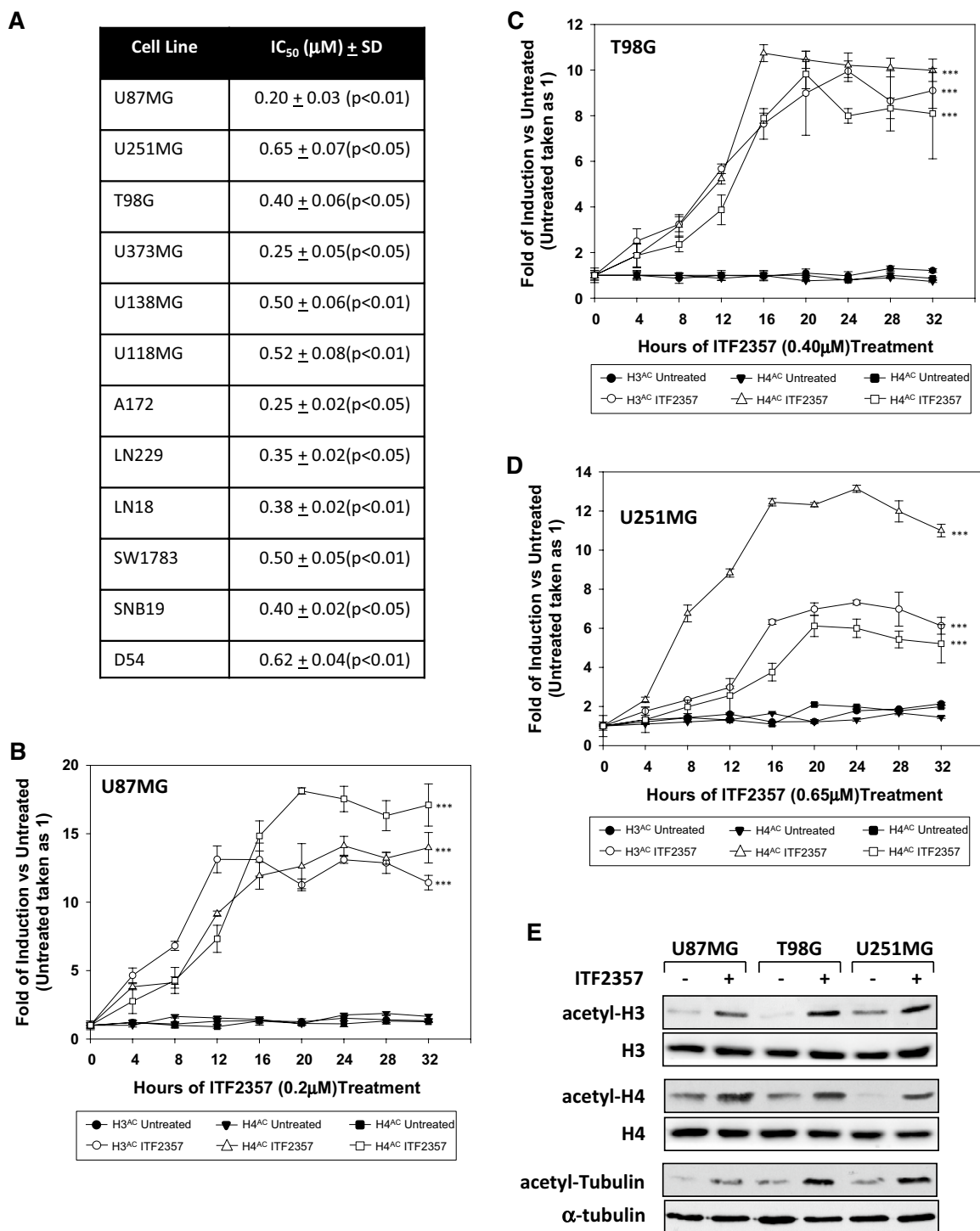


Fig. 1 ITF2357 affects HDACs' activity and GBM cell viability. **a** Dose of ITF2357 able to reduce, by 50%, the HDACs activation status of 12 GBM cell lines treated for 24 h with increasing doses of ITF2357 (0.1, 0.25, 0.5, 1, 2.5, and 5 μM). Results represent the mean values of four independent experiments ± SD. **b–d** Histone-H3 (H3), -H4 (H4), acetylated-Histone-H3 (H3^{AC}), -H4 (H4^{AC}), and α-tubulin (α-Tub^{AC}) were assessed on U87MG (**b**), T98G (**c**) and U251MG (**d**)

cell lines treated with the relative ITF2357 IC₅₀ dose for increasing time. Results represent the mean values of four independent experiments ± SD (Student's *t* test, **P* < 0.05; ***P* < 0.01; ****P* < 0.001). **e** Cell lysates from U87MG, T98G, and U251MG cells untreated (–) or treated (+) with ITF2357 (IC₅₀) for 24 h were analyzed by immunoblotting with specific antibodies for indicated proteins. Representative of four independent experiments

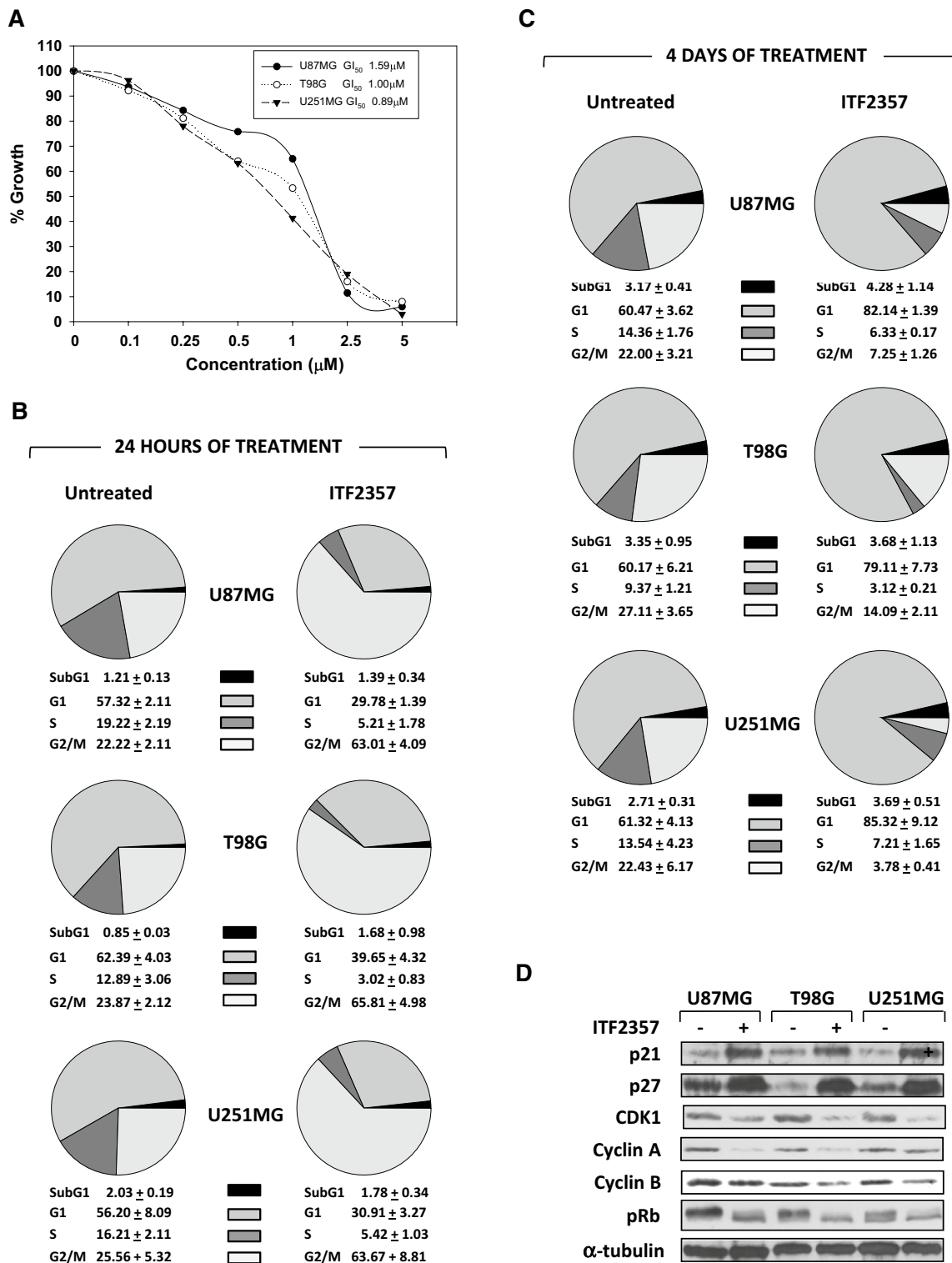


Fig. 2 Low doses of ITF2357 counteract GBM cell growth potential. **a** Dose of ITF2357 able to reduce by 50% the cell growth potential (GI_{50}) of U87MG, T98G, and U251MG cell lines treated with increasing doses of ITF2357 (GI_{50}) for 4 days. Results are representative of three independent experiments \pm SD. **b**, **c** FACS analysis performed on U87MG, T98G, and U251MG cell lines untreated or

treated with ITF2357 for 24 h (**b**) or 4 days (**c**). Results represent the mean value of three independent experiments \pm SD. **d** Cell lysates from U87MG, T98G, and U251MG cell lines treated for 4 days were analyzed by immunoblotting with specific antibodies for indicated proteins; α -Tubulin expression shows the loading of samples. Representative of three independent experiments

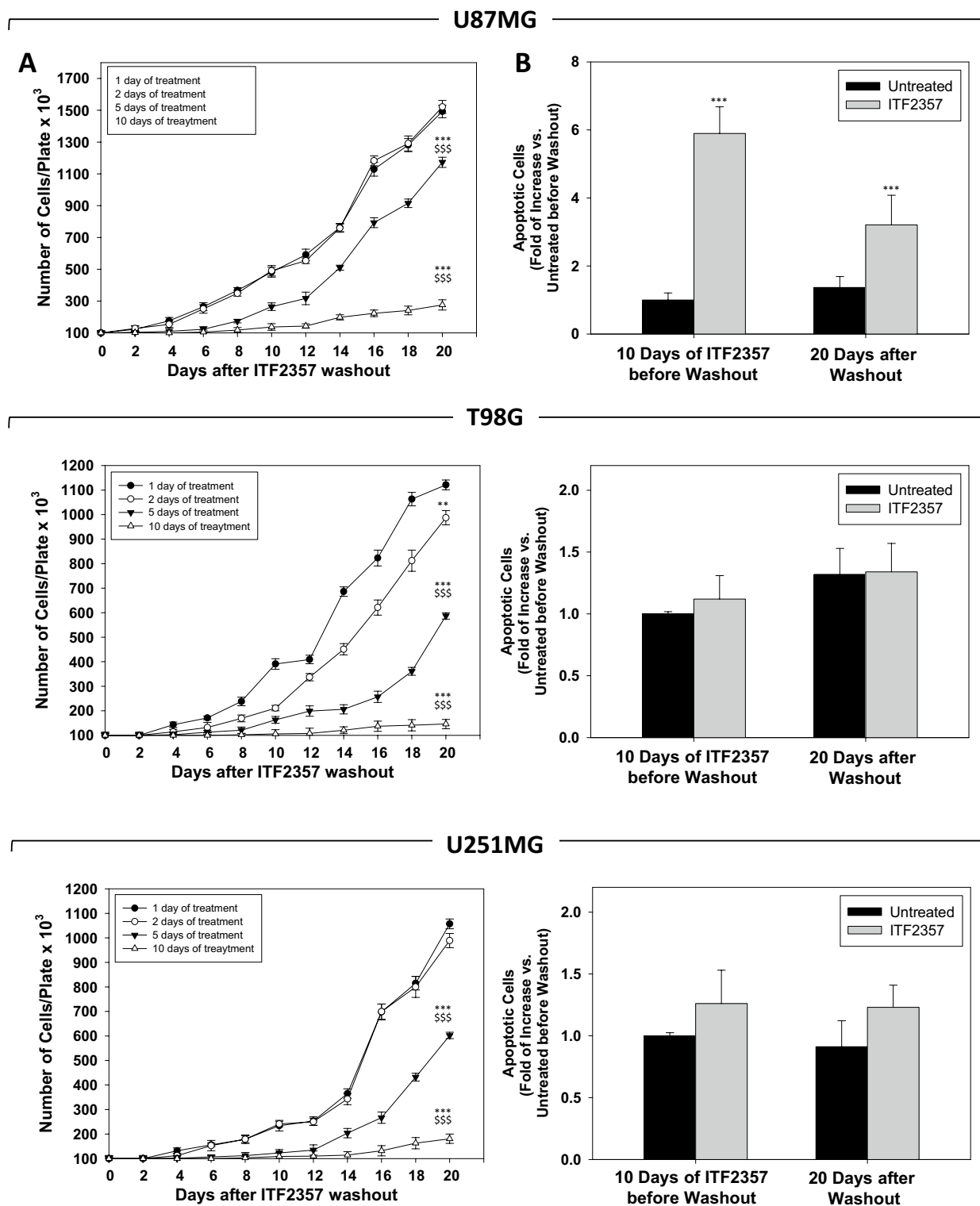


Fig. 3 Prolonged treatment with low-dose ITF2357 irreversibly affect GBM cell growth potential, concomitantly inducing U87MG cell death. **a** Outgrowth assay. U87MG, T98G, and U251MG cell lines were transiently (1, 2, 5, or 10 days) treated with ITF2357 (GI_{50} dose); growth medium-containing ITF2357 was washed-out and the cell count performed at the showed times. Results are representative

of three independent experiments \pm SD (Student's *t* test, $*P < 0.05$; $**P < 0.01$; $***P < 0.001$ vs. 1 day of ITF2357). **b** Percentage of dead cells on U87MG, T98G, and U251MG cell lines 10 days treated with ITF2357 (GI_{50} dose) and 20 days after the drug washout. Results are representative of three independent experiments \pm SD (Student's *t* test, $*P < 0.05$; $**P < 0.01$; $***P < 0.001$ vs. untreated)

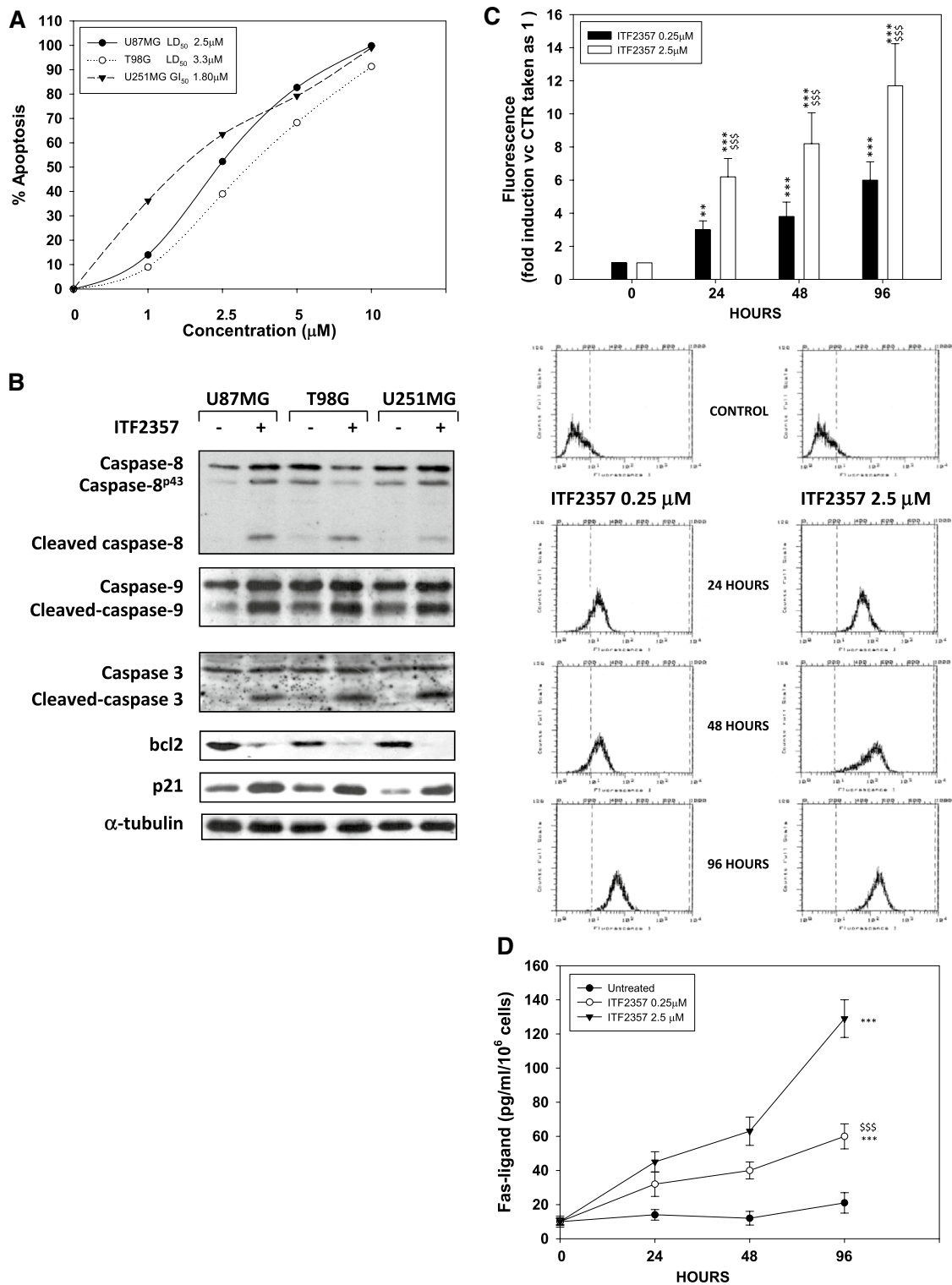
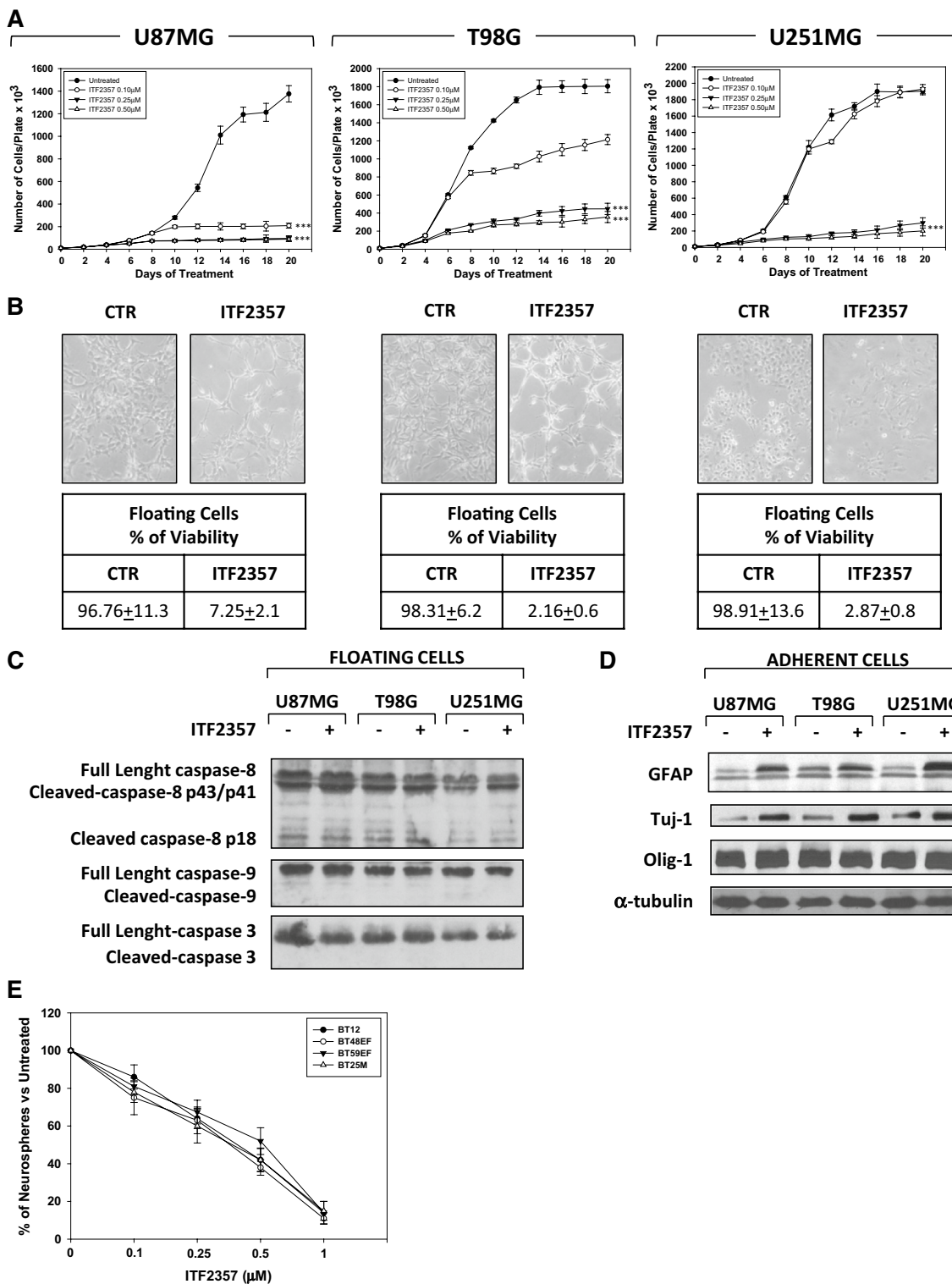


Fig. 4 High doses of ITF2357 induce GBM cell death. **a** Dose of ITF2357 able to induce 50% of cell death (LD₅₀) of U87MG, T98G, and U251MG cell lines treated with increasing doses of ITF2357 for 4 days. Results are representative of three independent experiments ± SD. **b** Cell lysates from U87MG, T98G, and U251MG cell lines treated for 24 h with the cell line relative LD₅₀ dose of ITF2357 were analyzed by immunoblotting with specific antibodies for indicated proteins; α-Tubulin expression shows the loading of samples.

Representative of three independent experiments. **c** Fas expression and **d** Fas-ligand secretion were assessed by FACS and ELISA, respectively, on U87MG cells treated with ITF2357 (0.25 μM or 2.5 μM) for increasing times. Results are representative of three independent experiments ± SD (Student's *t* test, **P* < 0.05; ***P* < 0.01; ****P* < 0.001 vs. untreated (0 h of treatment), ^S*P* < 0.05; ^{SS}*P* < 0.01; ^{SSS}*P* < 0.001 vs. 0.25 μM ITF2357)



ITF2357 able to induce 50% of cell growth inhibition (GI_{50}), the GI_{50} -related cell cycle distribution, and the modulation of the cell cycle regulators were investigated. After 4 days of ITF2357 treatment (0.1, 0.25, 0.5, 1, 2.5, 5, and 10 μ M), GI_{50} resulted $1.59 \pm 0.33 \mu$ M for U87MG, $1 \pm 0.21 \mu$ M for T98G, and $0.89 \pm 0.06 \mu$ M for U251MG cells (Fig. 2a).

Whether 24 h of ITF2357 (GI_{50}) treatment significantly increased G_2/M cellular fraction (Fig. 2b), the cell cycle distribution analysis performed 3 days later showed a significant increase of G_1/S cellular fraction (Fig. 2c), whilst no sub- G_1 apoptotic-relates events were detected both after 24 h (Fig. 2b) or 4 days (Fig. 2c) of ITF2357 treatment.

Fig. 5 Chronic treatment with low doses of ITF2357 induces growth arrest, non-apoptotic cell death, neuronal-like phenotype, and the expression of differentiation markers. **a** Cell count performed on U87MG, T98G, and U251MG cell lines daily treated for increasing times (0–20 days) with low doses of ITF2357 (0.1, 0.25, and 0.5 μ M). **b** Photomicrographs by contrast phase performed on U87MG, T98G, and U251MG cell lines daily treated for 20 days with ITF2357 (0.25 μ M). Representative of three independent experiments. **c, d** Cell lysates from floating (c) or adherent (d) U87MG, T98G, and U251MG cell lines daily treated for 20 days with ITF2357 (0.25 μ M) were analyzed by immunoblotting with specific antibodies for indicated proteins; α -Tubulin expression shows the loading of samples. Representative of three independent experiments. **e** Number of neurosphere formed by U87MG, T98G, and U251MG cell lines cultured on stem cells medium in the presence or absence of ITF2357 (0.1, 0.25, and 0.5 μ M) (Student's *t* test, * P < 0.05; ** P < 0.01; *** P < 0.001 vs. untreated)

At molecular level, ITF2357 upregulated the expression of the cell cycle inhibitors p21 and p27, downregulated the expression of positive cell cycle protein regulators CDK1, Cyclin A in U87MG and U251MG lines, and Cyclin B in T98G GBM cells (Fig. 2d). Furthermore, ITF2357 induced the hypophosphorylation of the retinoblastoma protein (pRb) in all the cell lines tested (Fig. 2c). Outgrowth assay showed that 10 days of transient exposure to ITF2357 $_{GI_{50}}$ dose drastically affected the ability of GBM cells to restore the proliferation rate ability (Fig. 3a); similar but lower effects were described in 1, 2, and 5 days transiently treated cells (Fig. 3a). The percentage of resulted U87MG apoptotic cells increased by 57.2 + 7.98% after 10 days of ITF2357 GI_{50} treatment and 23.2 + 8.3% 20 days after the washout (Fig. 3b, U87MG), while no significant modulations were described in T98G and U251MG cells (Fig. 3b, T98G and U251MG). The dose of ITF2357 able to induce 50% of lethal cell death (LD_{50}), determined 24 h after treatment, was 2.5 \pm 0.5 μ M in U87MG, 3.3 \pm 0.5 μ M in T98G, and 1.8 \pm 0.2 μ M in U251MG cells (Fig. 4a). ITF2357 LD_{50} dose induced the accumulation of cleaved-caspase 8, 9, and 3, Bcl2 down-regulation, and p21 up-regulation (Fig. 4b). We compared the surface expression of Fas by FACS (Fig. 4c) and Fas-ligand secretion by ELISA (Fig. 4d) on U87MG, showing an intermediate LD_{50} dose value. U87MG cells treated with ITF2357 0.25 μ M or 2.5 μ M (LD_{50}) for different times showed significant, rapid (24 h), and persistent (96 h) increased expression of Fas (Fig. 4c) and secretion of Fas ligand (Fig. 4d), which resulted directly in correlation with the used dose (0.25 μ M vs. 2.5 μ M, P < 0.001 Fas and P < 0.001 Fas ligand) at the end of the experiment (96 h) (Fig. 4d).

Chronic treatment with low doses of ITF2357 induces autophagy-related growth arrest, non-apoptotic cell death, neuronal-like phenotype, and expression of differentiation markers

GBM cells daily treated with low doses of ITF2357 (0.1, 0.25, and 0.5 μ M) showed a statistically significant growth arrest at 0.25 μ M (Fig. 5a). The lowest dose used (0.1 μ M) was able to inhibit U87MG by 85.6 + 13.1% and T98G cells by 43.2 + 11.7%, whilst no effects were described on U251MG cells (Fig. 5a). Administration of 0.5 μ M ITF2357 did not significantly improved 0.25 μ M-induced growth arrest (Fig. 5a). We noticed that, after 10 days of 0.25 μ M ITF2357 daily treatment, the number of floating cells increased, while adherent cells underwent towards relevant neuronal-like morphological changes (Fig. 5b, upper panel); contrary to adherent cells, floating cell was totally non-viable (Fig. 5b, Lower Panel). Cleaved-caspase 3, 8, and 9 assessed on floating cells resulted not modulated by treatment (Fig. 5c) that contrarily upregulated the expression of GFAP and Tuj-1 but not Olig-1 on adherent cells (Fig. 5d). Neurosphere formation assay was performed on four patient-derived GBM stem-cell lines (BT12, BT48EF, BT59EF, and BT52M) treated with increasing doses of ITF2357 (0.1, 0.25, 0.5, and 1 μ M). Fourteen days later, ITF2357 treatment restrained the ability to form neurosphere by 36.4 \pm 7.3% at 0.25 μ M, reaching 86.5 \pm 11.7% at 1 μ M the (Fig. 5e). Whether ITF2357 induced autophagy, known to promote GBM growth arrest, cell death, differentiation, and ability to counteract GBM stemness (Angeletti et al. 2016; Basile et al. 2018; Pawlowska et al. 2018; Zhuang et al. 2011) were investigated. As shown in Fig. 5a, 10 days of ITF2357 increased the expression levels of LC3II, beclin-1, ATG5, and ATG7 (Fig. 6a). Co-treatment with the autophagy inhibitor bafilomycin A (100 nM) significantly counteracted 0.25 μ M ITF2357-induced growth arrest by 56.3 \pm 8.32% in U87MG, 50.7 \pm 9.8% in T98G and 59.3.3 \pm 9.1% in U251MG cells (Fig. 6b) and restrained the ability of 10 days of 0.25 μ M of ITF2357 to increase the number of floating/dead cells by 64.5 \pm 11.6% in U87MG, 61.7 \pm 7.2% in T98G and 45.8 \pm 7.1% in U251MG cells (Fig. 6c). Furthermore, bafilomycin A significantly counteracted the accumulation of Tuj-1 differentiation marker in U87MG but not in T98G and U251MG cells (Fig. 6c). The ability of bafilomycin A to efficiently inhibit the autophagic flux was verified by LC3 western blot (Fig. 6c).

ITF2357 efficiently crosses the blood–brain barrier, induces brain tissue hyper-acetylation, and counteracts in vivo tumor growth

The ability of ITF2357 to cross the blood–brain barrier and induce HDACi-mediated histone acetylation was

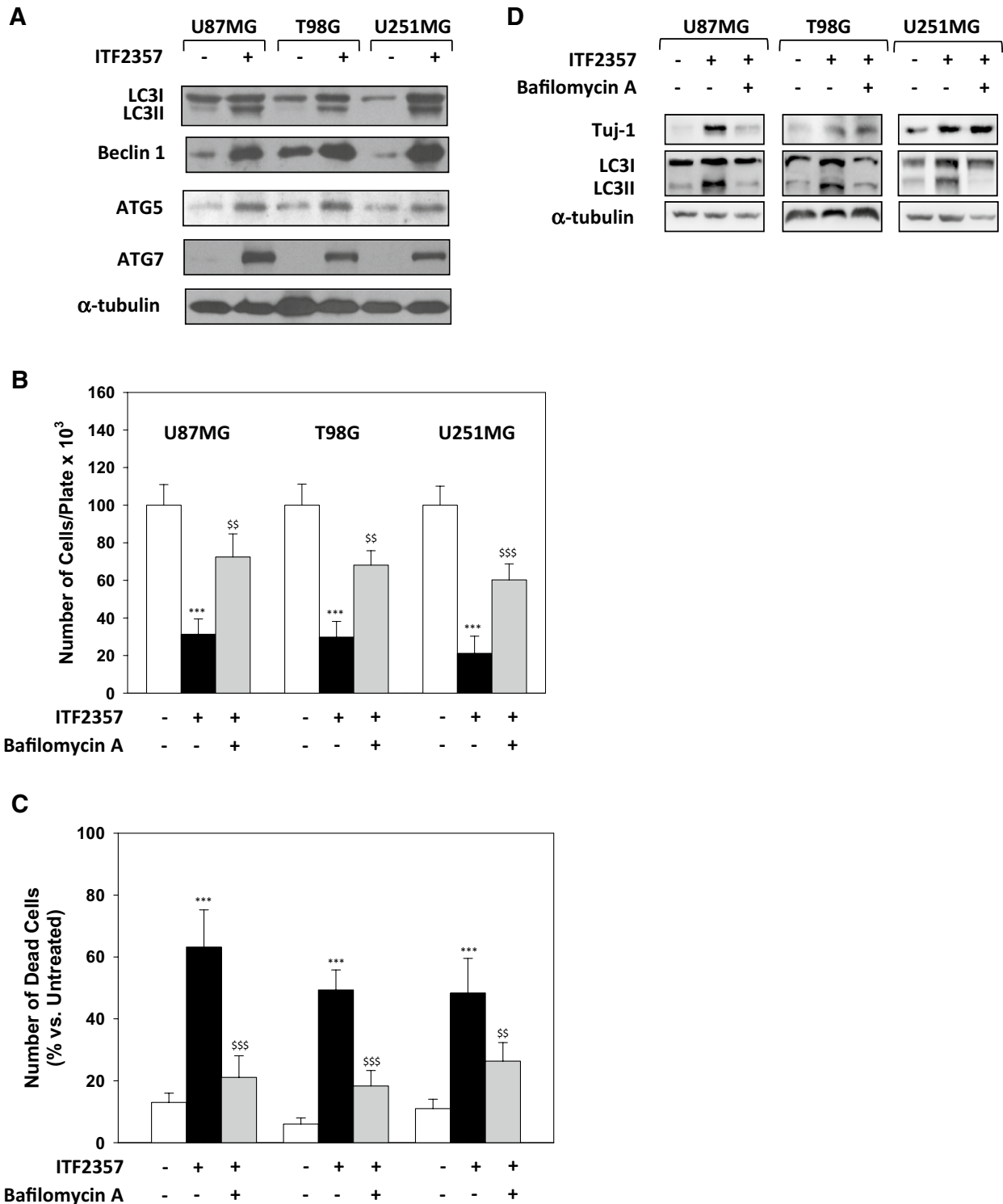


Fig. 6 Chronic treatment with low doses of ITF2357 induces autophagy, responsible of treatment-mediated cell death and U87MG differentiation. **a** Cell lysates from U87MG, T98G, and U251MG cell lines daily treated for 10 days with ITF2357 (0.25 μM) were analyzed by immunoblotting with specific antibodies for indicated proteins; α-Tubulin expression shows the loading of samples. **b**, **c** U87MG, T98G, and U251MG cell lines were daily treated for 10

days with ITF2357 (0.25 and 0.5 μM) in the presence or absence of bafilomycin A (100 nM). At the end of the experiments, live (**b**) and dead (**c**) cells were counted (Student's *t* test, **P*<0.05; ***P*<0.01; ****P*<0.001 vs. untreated, ^{\$}*P*<0.05; ^{\$\$}*P*<0.01; ^{\$\$\$}*P*<0.001 vs. 0.25 μM ITF2357). **d** Cell lysates were analyzed by immunoblotting with specific antibodies for indicated proteins; α-Tubulin expression shows the loading of samples

investigated on brains collected from rat orally treated with 50 and 100 mg/kg of ITF2357 for 1, 3, or 6 h. As shown in Fig. 7a, ITF2357 increased acetylation of H3 in a dose- and time-dependent manner having a statistically significant increase after 3 h from the treatment that reached the highest level 3 h later (Fig. 7a). The effects of ITF2357 on in vivo tumor growth were investigated on forty 5-week-old female CD1 nude mice xenotransplanted with U87MG or U251MG cells. After tumors became measurable, animals were randomized in four groups of ten mice each, to receive vehicle, 0.1 mg/kg, 1 mg/kg, or 10 mg/kg bi-daily; treatment was administered by oral gavage two times a day and performed 5 days a week for 7 weeks, and tumor sizes were measured weekly for 70 days (See schematization Upper Fig. 7b). ITF2357 counteracted tumor growth in a dose-dependent manner (Fig. 7b). On U87MG xenografted mice (Fig. 7b, Left Panel), 0.1 mg/kg delayed the end point 1 by 10 days, while, in 1 or 10 mg/kg treated mice, volume reached $830 + 65 \text{ mm}^3$ or $530 + 56 \text{ mm}^3$, respectively, affecting tumor growth by 44.6% (0.1 mg/kg) or 64.6% (1 mg/kg) (Fig. 7b). On U251MG xenografted mice (Fig. 7b, right panel), 0.1 mg/kg delayed the end point 1 by 15 days, while, in 1 mg/kg or 10 mg/kg treated mice, volume reached $1043 + 93 \text{ mm}^3$ or $762 + 101 \text{ mm}^3$, respectively, thus affecting by 31.3% (1 mg/kg) or 49.3% (10 mg/kg) tumor growth (Fig. 7c). The mean tumor weight was calculated for each treatment group. Figure 7c shows that ITF2357 was able to reduce tumor weight in a dose-dependent manner in U87MG (Fig. 7c, left panel) and U251MG (Fig. 7c, right panel) xenografts. Statistically significant differences were observed between the vehicle control groups and the groups treated with ITF2357 at 1 and 10 mg/kg (Fig. 7c). To reduce the probability of an error due to the tumor volume at the start of drug administration, we compared the Time-to-Progression (TTP) defined as the time (days) necessary to double the tumor volume for each tumor. ITF2357-treated mice had a significantly delayed median time-to-progression in a dose-dependent manner, in both the xenografted cells lines (Fig. 8a, U87MG and Fig. 8b, U251MG), as shown by post hoc analysis (Dwass–Steel–Critchlow–Fligner method).

Conclusions

Glioblastoma are the most common and lethal intracranial tumors (Johnson and O’Neill 2012). Herein, using a cohort of GBM cell lines and patient-derived glioma stem cells, we show that ITF2357 (givinostat), a pan-HDAC inhibitor (HDACi) with an anti-inflammatory (Leoni et al. 2005), anti-angiogenic (Golay et al. 2007), and anti-neoplastic activities (Golay et al. 2007; Topper et al. 2017) counteracts GBM oncophenotype by inducing a dose-dependent: (1) cell cycle arrest; (2) apoptosis; (3) autophagy-related

non-apoptotic cell death and differentiation; (4) reduction on GBM stemness potential. Furthermore, ITF2357 impaired in vivo GBM growth on xenograft mouse models.

HDACi have been shown to induce G_1 or G_2/M growth arrest or death in different cell types (Glozak and Seto 2008) by, respectively, modulating the expression of several cell cycle regulators or the activation of several apoptotic mediators (Newbold et al. 2016). Regarding the ability to induce growth arrest, herein, we found that doses of ITF2357 between 1 and $2.5 \mu\text{M}$ -induced G_1/S cell cycle growth arrest, whilst the activation of the apoptotic program for doses was higher than $2.5 \mu\text{M}$. ITF2357 has been already shown to induce G_1 cell cycle growth arrest in several cancer cell lines (Zappasodi et al. 2008, 2014; Yao et al. 2017). Furthermore, the G_1/S arrest was preceded by a transitory accumulation of cells in the G_2 phase of the cell cycle and why GBM cells resulted initially blocked at G_2/M but subsequently arrested in the G_1/S phase of the cell cycle, needs to further investigations. According to the molecular mechanisms known to control the G_1/S checkpoint, we found that ITF2357 upregulated the expression of p21 and p27, down-regulated of CDK1, cyclin A, and cyclin B, and induced the hypophosphorylation/inhibition of the retinoblastoma protein (Bertoli et al. 2013). Interestingly, we also found that the prolonged treatments with ITF2357 induced an irreversible growth arrest, indicating that the effects induced by ITF2357 are not reversible. The prolonged cell cycle arrest has been shown to trigger the activation of apoptosis; this results in DNA damage and p53 induction (Orth et al. 2012). Herein, by assessing apoptosis 10 days after ITF2357 treatment and 20 days after the washout, we found that the percentage of GBM apoptotic cells resulted increased in U87MG but not in T98G and U251MG cell lines. It has been shown that the HDACi trichostatin A induces p53-dependent anti-proliferative and pro-apoptotic effects of in U87MG cells. U87MG differs from T98G and U251MG cells for the expression of the wild-type form of p53 (Van Meir et al. 1994). Thus, the effects of ITF2357 prolonged treatment in inducing irreversible growth arrest seem to be related to the activation of the apoptotic program; the mechanisms activated by ITF2357 in the p53 mutant T98G and U251MG cells remain unknown and the activation of non-death programs such as senescence or differentiation can be hypothesized. For the induced cell cycle arrest, the molecular pattern characterizing ITF2357-induced GBM apoptosis resumed what already showed in other cancer cells (Galimberti et al. 2010), with a full activation of both the intrinsic caspase 9- and extrinsic caspase 8-mediated apoptotic pathways. Upon binding of FasL, Fas complexes with FADD (Fas-associated with a death domain), procaspase-8, procaspase-10, and c-FLIP, this promotes caspase-8 activation and results in the execution of extrinsic apoptosis program (Medema et al. 1997). The intrinsic pathway acts in response to death stimuli, including

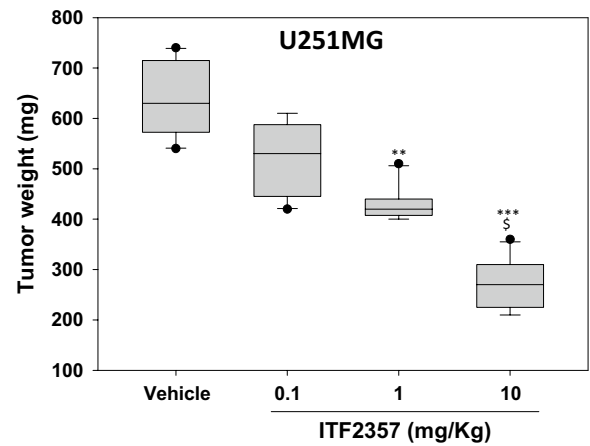
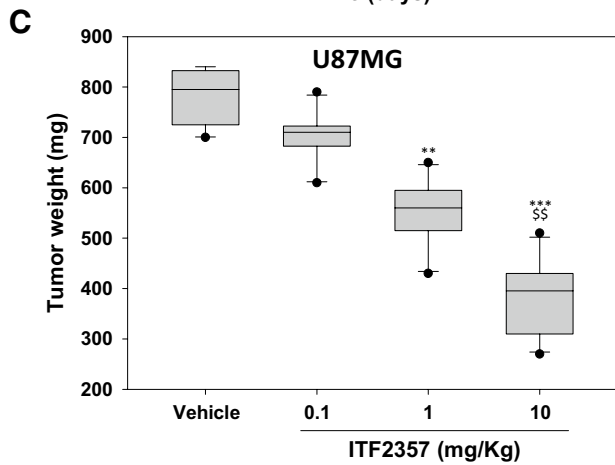
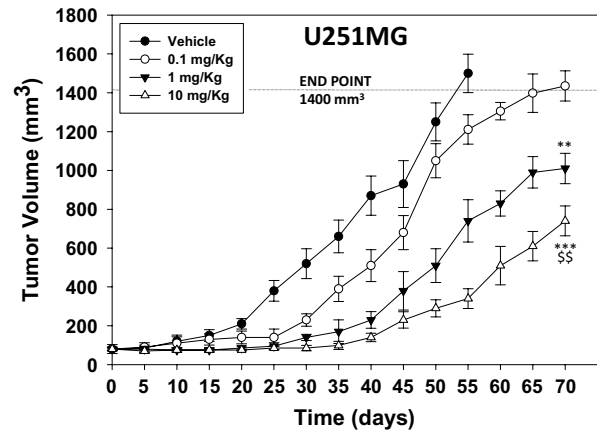
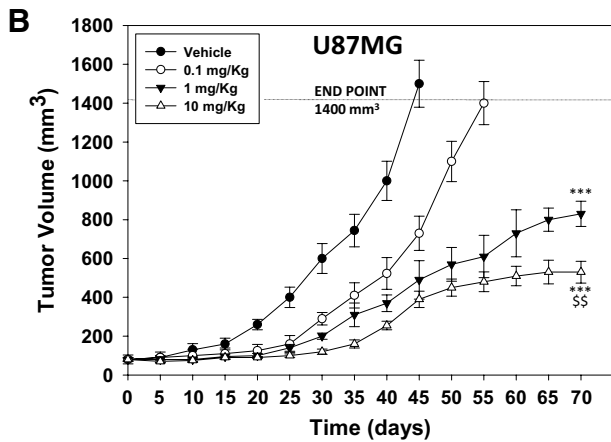
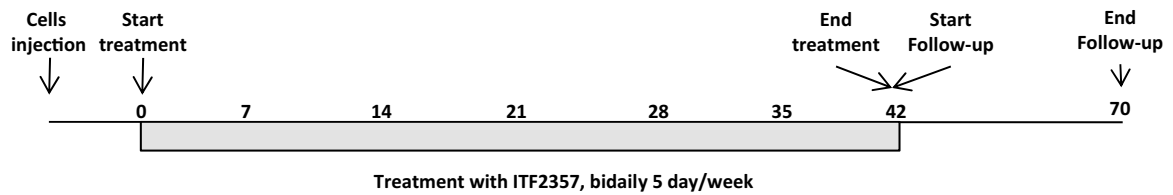
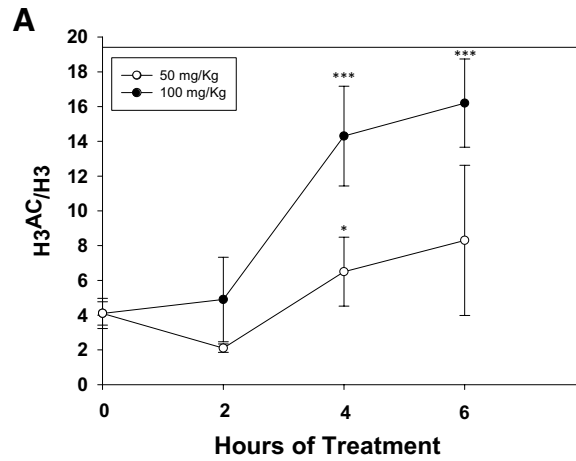


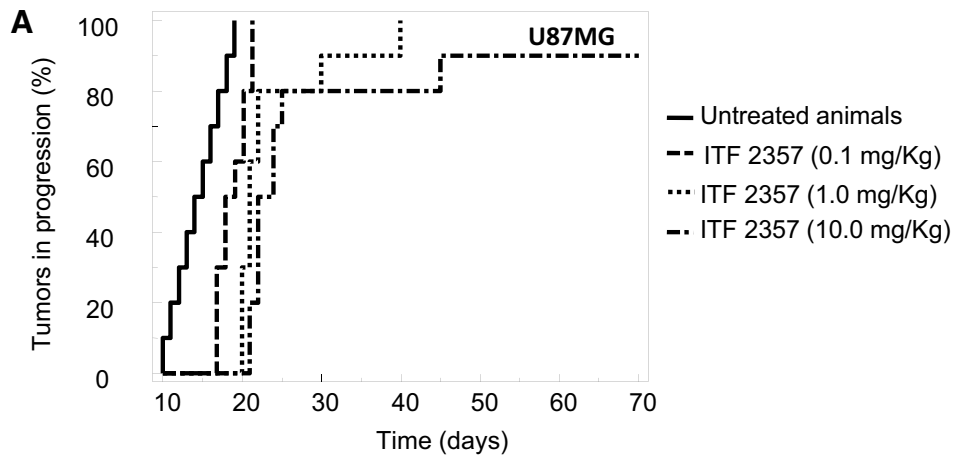
Fig. 7 ITF2357 efficiently crosses the blood–brain barrier (BBB), induces brain tissue hyper-acetylation, and counteracts GBM growth in vivo. **a** Data in the scatter plot curves represent the densitometric analysis of western blots performed on brain tissue from rats orally treated with 50 and 100 mg/kg of ITF2357 and sacrificed 1, 3, or 6 h after treatment (Student's *t* test, * $P < 0.05$; ** $P < 0.01$; *** $P < 0.001$ vs. Untreated). **b** Tumor volume and **c** tumor weight from U87MG and U251MG cells in xenografted mice bi-daily treated with 0.1 mg/kg, 1 mg/kg, or 10 mg/kg. Bars represent mean \pm SD. Statistical significance is indicated (Student's *t* test, * $P < 0.05$; ** $P < 0.01$; *** $P < 0.001$ vs. untreated)

chemotherapeutic agent-mediated mitochondrial DNA damage (Wang and Youle 2009), and can cross talk with the extrinsic pathway through caspase-8 mediated cleavage of Bid, which translocates to mitochondria and triggers cytochrome c release (Li et al. 1998). Herein, we found that ITF2357 induced a full activation of the apoptotic pathways, but it remains to understand if the intrinsic pathway activation resulted directly from ITF2357 action or was mediated by extrinsic pathway activation, as we suppose.

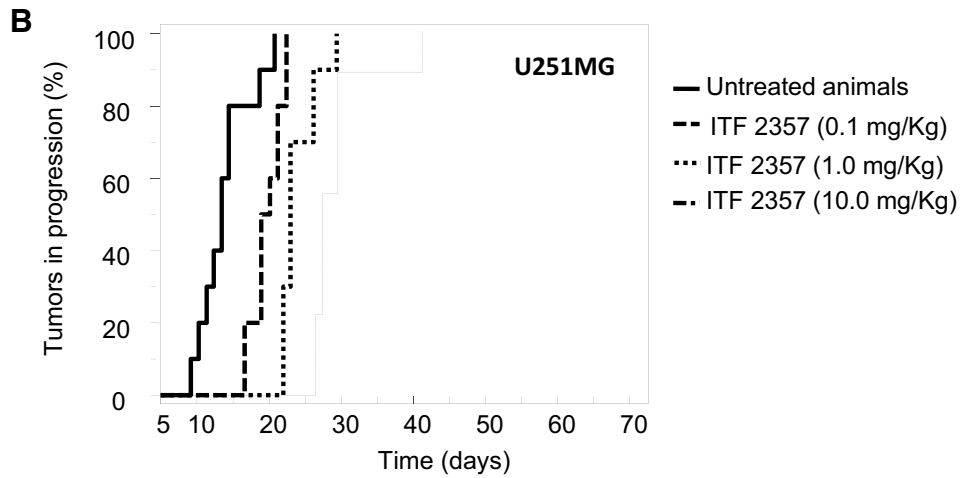
By investigating on the effects of chronic drug treatment at low doses, we noticed that ITF2357 increased the percentage of floating dead cells without affecting the caspases activation status and induced neuronal-like morphological changes, associated with the expression of GFAP and Tuj-1 neuronal differentiation markers, in attached-surviving cells. Whether the ability of ITF2357 to induce differentiation markers was in line with already collected evidences (Svechnikova et al. 2008), it remained to understand how chronic low dose of treatment induced cell death, considering that various non-apoptotic forms of cell death also exist (Tait et al. 2014). Autophagy, a lysosome-dependent process that degrades molecules and organelles, can induce cell death (autophagic or type II cell death) through the activation of apoptotic or non-apoptotic pathway (Rubinstein and Kimchi 2012). It has been recently showed that autophagy restrains the cytotoxic activity of ITF2357 (Angeletti et al. 2016) and promotes the differentiation of human GBM cells (Basile et al. 2018; Pawlowska et al. 2018; Zhuang et al. 2011). Thus, we supposed that chronic low dose of ITF2357 by inducing the activation of the autophagic program was able to simultaneously promote cell death and differentiation. Founding that the chronic treatment with low doses of ITF2357 increased the levels of LC3-II (Tanida et al. 2008), Beclin1-, ATG5-, and ATG7-autophagy-related-proteins (Kang et al. 2011), suggested the autophagy as the potential mechanism responsible for the ITF2357-induced cell death and differentiation. This suggestion was confirmed using the autophagy inhibitor bafilomycin A that restrained the ability of ITF2357 to induce cell death in all the cell lines tested and the expression of Tuj-1 differentiation marker in U87MG but not in T98G and U251MG cells. Surprisingly, the co-treatment with bafilomycin A decreases LC3-II levels, when

it should result in a higher amount as a consequence of the inhibition of the autophagosome-lysosome fusion step (Klionsky et al. 2012, 2016; Mizushima et al. 2007). Treatment with bafilomycin A is usually performed for few hours or days and not for longer treatment, such as 10 days. At now, we can just suppose that, after a prolonged treatment, ITF2357 could interact with bafilomycin A promoting competitive effects or that GBM cancer cells, when chronically treated, can develop a resistance to bafilomycin A, ability already shown in other cell lines (Tanigaki et al. 2003). However, whatever the mechanism, this does not seem to be able to revert the anti-autophagic signal initially triggered by bafilomycin A and able to counteract the apoptosis and differentiation triggered by ITF2357. Further experiments will be performed to characterize this phenomenon. Finally, we speculate on the ability of bafilomycin A to restrain the expression of Tuj-1 differentiation marker in p53 expressing U87MG but not in p53-null T98G and U251MG cells. p53 has been shown to control neural and glioma cell differentiation (Zheng et al. 2008) and to play a key role in regulating autophagy (Eileen et al. 2016). In light of the collected data, we can assume that ITF2357 is able to activate the differentiation program in a p53 dependent or independent manner and that in p53-expressing cells, but not in p53-null cells, this process is autophagy mediated. Future investigations will be performed to understand which mechanisms promote p53-independent differentiation.

A drug capable of inducing differentiation is supposed to be able to disadvantage the phenotype of undifferentiated cancer stem cells, that presenting a self-renewal and multi-lineage differentiation capacity as well as a long-term proliferative, which have been shown to play a pivotal role in the initiation and progression of cancers (Bakhshinyan et al. 2018). Particularly, this uncontrolled renewal potential of CSCs might be the reason for tumor relapse after the conventional cancer therapies (Bakhshinyan et al. 2018). Although multiple drugs were found to affect the phenotype of the tumor mass, the efficacy of these drugs was limited and did not affect the tumor-initiating cells. Our results using the neurosphere growth assay provide evidence that HDAC inhibition by ITF2357 suppresses the survival or growth of GBM stem cells by counteracting the neurosphere formation. Based on these observations, we decided to investigate the effect of ITF2357 on an in vivo GBM tumor model. The U87MG and U251MG cell lines were xenotransplanted using the highest cellular concentration (1×10^7 cells per mouse) to achieve maximum tumor uptake (100%) and large tumors to reproduce the unfavorable conditions required to effectively test an anti-tumor drug. Indeed, ITF2357 significantly reduced the growth of xenotransplanted tumors, delaying the tumor progression. Moreover, in the perspective of the clinical use of ITF2357 for GBM treatment, it is important to note that this compound is able to cross the



	Vehicle vs 0.1 mg/Kg	Vehicle vs 1.0 mg/Kg	Vehicle vs 10.0 mg/Kg
HR	2.85	6.86	9.20
CI95%	0,75 to 6.52	1.47 to 13.44	2.29 to 18.45
significance	P=0.0134	P<0.0001	P<0.0001



	Vehicle vs 0.1 mg/Kg	Vehicle vs 1.0 mg/Kg	Vehicle vs 10.0 mg/Kg
HR	2.14	4,87	6.68
CI95%	0.65 to 5,82	1.25 to 10.88	2.18 to 12.87
significance	P=0.0255	P<0.0001	P<0.0001

Fig. 8 Time-to-Progression analysis from GBM xenografted mice treated with ITF2357. **a** Analysis of tumor development by Dwass–Steel–Critchlow–Fligner method

BBB, at least in the rat, and to inhibit HDAC activities, as indicated by the increase of histones acetylation in the brain tissue.

Therapeutic strategies able to induce cell death and differentiation are an ideal strategy in cancer therapy and have been successfully applied in the treatment of leukemia (Petrie et al. 2009). Thus, ITF2357, by acting as a cytotoxic or a cytostatic/differentiating drug, may be used in an epigenetic-based therapy for GBM and warrant testing in pre-clinical and clinical GBM trials.

Acknowledgements We are grateful to the Umberto Veronesi Foundation for awarding a post-doctoral fellowship to Francesco Marampon for the year 2018 and “FIVA Confcommercio” for supporting part of our work. ITF2357 was provided by Italfarmaco SpA.

Author contributions FMa and FL planned experiments; AM, IP, SDM, SC, FMe GP, EG, and PP performed experiments; AB, PM, RM, and VT analyze data; GLG and CF wrote the paper.

Compliance with ethical standards

Conflict of interest Giuliana Porro, Elisabetta Galbiati, Pietro Pozzi, and Paolo Mascagni are employers of ItalfarmacoSpA. The other authors declare that they have no competing interests.

Ethical approval Studies on animal models were performed according to the guidelines established by the University of L’Aquila, Medical School and Science and Technology School Board Regulations, in compliance with the Italian government regulation no. 116 January 27, 1992 and national/international guidelines for the care and use of animals. The present study was approved by the Ethical Committee of the Medical School of the University of L’Aquila, (555/2017-PR). This article does not contain any studies with human participants performed by any of the authors.

Informed consent This article does not contain any studies with human participants performed by any of the authors.

References

Angeletti F, Fossati G, Pattarozzi A, Würth R, Solari A, Daga A, Masiello I, Barbieri F, Florio T, Comincini S (2016) Inhibition of the autophagy pathway synergistically potentiates the cytotoxic activity of givinostat (ITF2357) on human glioblastoma cancer stem cells. *Front Mol Neurosci* 9:107

Bakhshinyan D, Adile AA, Qazi MA, Singh M, Kameda-Smith MM, Yelle N, Chokshi C, Venugopal C, Singh SK (2018) Introduction to cancer stem cells: past, present, and future. *Methods Mol Biol* 1692:1–16

Basile MS, Mazzon E, Krajnovic T, Draca D, Cavalli E, Al-Abed Y, Bramanti P, Nicoletti F, Mijatovic S, Maksimovic-Ivanic D (2018) Anticancer and differentiation properties of the nitric oxide derivative of lopinavir in human glioblastoma cells. *Molecules* 26:23

Bertoli C, Skotheim JM, de Bruin RA (2013) Control of cell cycle transcription during G1 and S phases. *Nat Rev Mol Cell Biol* 14(8):518–28

Bezacny P (2014) Histone deacetylase inhibitors in glioblastoma: pre-clinical and clinical experience. *Med Oncol* 31:985

Chen HP, Zhao YT, Zhao TC (2015) Histone deacetylases and mechanisms of regulation of gene expression. *Crit Rev Oncog* 20:35–47

Cusulin C, Chesnelong C, Bose P, Bilenky M, Kopciuk K, Chan JA, Cairncross JG, Jones SJ, Marra MA, Luchman HA, Weiss S (2015) Precursor states of brain tumor initiating cell lines are predictive of survival in xenografts and associated with glioblastoma subtypes. *Stem Cell Reports* 5:1–9

De Souza C, Chatterji BP (2015) HDAC Inhibitors as Novel Anti-Cancer Therapeutics. *Recent Pat Anticancer Drug Discov* 10:145–162

Eckschlager T, Plch J, Stiborova M, Hrabeta J (2017) Histone deacetylase inhibitors as anticancer drugs. *Int J Mol Sci* 18:E1414

Eileen W (2016) Autophagy and p53. *Cold Spring Harb Perspect Med* 6:a026120

Festuccia C, Mancini A, Colapietro A, Gravina GL, Vitale F, Marampon F, DelleMonache S, Pompili S, Cristiano L, Vetuschi A, Tombolini V, Chen Y, Mehrling T (2018) The first-in-class alkylating deacetylase inhibitor molecule tinostamustine shows antitumor effects. *J HematolOncol* 11:32

Galimberti S, Canestraro M, Savli H, Palumbo GA, Tibullo D, Nagy B, Piaggi S, Guerrini F, Cine N, Metelli MR, Petrini M (2010) ITF2357 interferes with apoptosis and inflammatory pathways in the HL-60 model: a gene expression study. *Anticancer Res* 30:4525–4535

Glozak MA, Seto E (2008) Histone deacetylases and cancer. *Oncogene* 26:5420–5432

Golay J, Cuppini L, Leoni F, Micò C, Barbui V, Domenghini M, Lombardi L, Neri A, Barbui AM, Salvi A, Pozzi P, Porro G, Pagani P, Fossati G, Mascagni P, Inrona M, Rambaldi A (2007) The histone deacetylase inhibitor ITF2357 has anti-leukemic activity in vitro and in vivo and inhibits IL-6 and VEGF production by stromal cells. *Leukemia* 21:1892–1900

Johnson DR, O’Neill BP (2012) Glioblastoma survival in the United States before and during the temozolomide era. *J Neurooncol* 107:359–364

Kang J, Shi Y, Xiang B, Qu B, Su W, Zhu M, Zhang M, Bao G, Wang F, Zhang X, Yang R, Fan F, Chen X, Pei G, Ma L (2005) A nuclear function of beta-arrestin1 in GPCR signaling: regulation of histone acetylation and gene transcription. *Cell* 123:833–847

Kang R, Zeh HJ, Lotze MT, Tang D (2011) The Beclin 1 network regulates autophagy and apoptosis. *Cell Death Differ* 18:571–580

Kelly JJ, Stechishin O, Chojnacki A, Lun X, Sun B, Senger DL, Forsyth P, Auer RN, Dunn JF, Cairncross JG, Parney IF, Weiss S (2009) Proliferation of human glioblastoma stem cells occurs independently of exogenous mitogens. *Stem Cells* 27:1722–1733

Klionsky DJ et al (2012) Guidelines for the use and interpretation of assays for monitoring autophagy. *Autophagy* 8:445–544

Klionsky DJ et al (2016) Guidelines for the use and interpretation of assays for monitoring autophagy (3rd edn). *Autophagy* 12:1–222

Legube G, Trouche D (2003) Regulating histone acetyltransferases and deacetylases. *EMBO Rep* 4:944–947


Leoni F, Fossati G, Lewis EC, Lee JK, Porro G, Pagani P, Modena D, Moras ML, Pozzi P, Reznikov LL, Siegmund B, Fantuzzi G, Dinarello CA, Mascagni P (2005) The histone deacetylase inhibitor ITF2357 reduces production of pro-inflammatory cytokines in vitro and systemic inflammation in vivo. *Mol Med* 11:1–15

Li H, Zhu H, Xu CJ, Yuan J (1998) Cleavage of BID by caspase 8 mediates the mitochondrial damage in the Fas pathway of apoptosis. *Cell* 94:491–501

Marampon F, Gravina GL, Zani BM, Popov VM, Fratticci A, Cerasani M, Di Genova D, Mancini M, Ciccarelli C, Ficorella C, Di Cesare E, Festuccia C (2014) Hypoxia sustains

- glioblastoma radioresistance through ERKs/DNA-PKcs/HIF-1 α functional interplay. *Int J Oncol* 44:2121–2131
- Marampon F, Gravina GL, Ju X, Vetuschi A, Sferra R, Casimiro MC, Pompili S, Festuccia C, Colapietro A, Gaudio E, Di Cesare E, Tombolini V, Pestell RG (2016) Cyclin D1 silencing suppresses tumorigenicity, impairs DNA double strand break repair and thus radiosensitizes androgen-independent prostate cancer cells to DNA damage. *Oncotarget* 7:5383–5400
- Marampon F, Megiorni F, Camero S, Crescioli C, McDowell HP, Sferra R, Vetuschi A, Pompili S, Ventura L, De Felice F, Tombolini V, Dominici C, Maggio R, Festuccia C, Gravina GL (2017) HDAC4 and HDAC6 sustain DNA double strand break repair and stem-like phenotype by promoting radioresistance in glioblastoma cells. *Cancer Lett* 397:1–11
- Medema JP, Scaffidi C, Kischkel FC, Shevchenko A, Mann M, Krammer PH, Peter ME (1997) FLICE is activated by association with the CD95 death-inducing signaling complex (DISC). *EMBO J* 16:2794–2804
- Mizushima N (2007) Autophagy: process and function. *Genes Dev* 21:2861–2873
- Nagarajan RP, Costello JF (2009) Molecular epigenetics and genetics in neuro-oncology. *Neurotherapeutics* 6:436–446
- Newbold A, Falkenberg KJ, Prince HM, Johnstone RW (2016) How do tumor cells respond to HDAC inhibition? *FEBS J* 283:4032–4046
- Orth JD, Loewer A, Lahav G, Mitchison TJ (2012) Prolonged mitotic arrest triggers partial activation of apoptosis, resulting in DNA damage and p53 induction. *Mol Biol Cell* 23:567–576
- Pawlowska E, Szczepanska J, Szatkowska M, Blasiak J (2018) An Interplay between senescence, apoptosis and autophagy in glioblastoma multiforme—role in pathogenesis and therapeutic perspective. *Int J Mol Sci* 17:19
- Petrie K, Zelent A, Petrie K, Zelent A, Waxman S (2009) Differentiation therapy of acute myeloid leukemia: past, present and future. *Curr Opin Hematol* 16:84–91
- Rosanò L, Cianfrocca R, Tocci P, Spinella F, Di Castro V, Spadaro F, Salvati E, Biroccio AM, Natali PG, Bagnato A (2013) β -arrestin-1 is a nuclear transcriptional regulator of endothelin-1-induced β -catenin signaling. *Oncogene* 32:5066–5077
- Rubinstein AD, Kimchi (2012) A Life in the balance - a mechanistic view of the crosstalk between autophagy and apoptosis. *J Cell Sci* 125:5259–5268
- Sferra R, Pompili S, Festuccia C, Marampon F, Gravina GL, Ventura L, Di Cesare E, Cicchinelli S, Gaudio E, Vetuschi A (2017) The possible prognostic role of histone deacetylase and transforming growth factor β /Smad signaling in high grade gliomas treated by radio-chemotherapy: a preliminary immunohistochemical study. *Eur J Histochem* 61:2732
- Song Q, Ji Q, Li Q (2018) The role and mechanism of β arrestins in cancer invasion and metastasis. *Int J Mol Med* 41:631–639
- Svechnikova I, Almqvist PM, Ekström TJ (2008) HDAC inhibitors effectively induce cell type-specific differentiation in human glioblastoma cell lines of different origin. *Int J Oncol* 32:821–827
- Tait SW, Ichim G, Green DR (2014) Die another way—non-apoptotic mechanisms of cell death. *J Cell Sci* 127:2135–2144
- Tanida I, Ueno T, Kominami E (2008) LC3 and autophagy. *Methods Mol Biol* 445:77–88
- Tanigaki K, Sasaki S, Ohkuma S (2003) In bafilomycin A1-resistant cells, bafilomycin A1 raised lysosomal pH and both prodiginosins and concanamycin A inhibited growth through apoptosis. *FEBS* 537:79–84
- Topper MJ, Vaz M, Chiappinelli KB, DeStefano Shields CE, Niknafs N, Yen RC, Wenzel A, Hicks J, Ballew M, Stone M, Tran PT, Zahnow CA, Hellmann MD, Anagnostou V, Strissel PL, Strick R, Velculescu VE, Baylin SB (2017) Epigenetic therapy ties MYC depletion to reversing immune evasion and treating lung cancer. *Cell* 171:1284–1300.e21
- Van Meir EG, Kikuchi T, Tada M, Li H, Diserens AC, Wojcik BE, Huang HJ, Friedmann T, de Tribolet N, Cavenee WK (1994) Analysis of the p53 gene and its expression in human glioblastoma cells. *Cancer Res* 54:649–52
- Vulcano F, Ciccarelli C, Mattia G, Marampon F, Giampiero M, Milazzo L, Pascuccio M, Zani BM, Giampaolo A, Hassan HJ (2006) HDAC inhibition is associated to valproic acid induction of early megakaryocytic markers. *Exp Cell Res* 312:1590–1597
- Wang C, Youle RJ (2009) The role of mitochondria in apoptosis. *Annu Rev Genet* 43:95–118
- Yao C, Zhang G, Walker A, Zhao KY, Li Y, Lyu L, Tang Y, Ru P, Jones D, Zhao W (2017) Potent induction of apoptosis by givinostat in BCR-ABL1-positive and BCR-ABL1-negative precursor B-cell acute lymphoblastic leukemia cell lines. *Leuk Res* 60:129–134
- Yoshida M, Kijima M, Akita M, Beppu T (1990) Potent and specific inhibition of mammalian histone deacetylase both in vivo and in vitro by trichostatin A. *J Biol Chem* 265:17174–17179
- Zappasodi MDR, Nicola F, Baldan MV, Iorio M, Magni E, Tagliabue CM, Croce, and Alessandro M, Gianni (2008) Carmelo Carlo-Stella. Cytotoxic activity of histone deacetylase inhibitor ITF2357 on Burkitt's Lymphoma Cell Lines Is Associated to Micro-RNA Modulation and Transglutaminase 2 Restoration. *Blood* 112:1594
- Zappasodi R, Cavanè A, Iorio MV, Tortoreto M, Guarnotta C, Ruggiero G, Piovan C, Magni M, Zaffaroni N, Tagliabue E, Croce CM, Zunino F, Gianni AM, Di Nicola M (2014) Pleiotropic antitumor effects of the pan-HDAC inhibitor ITF2357 against c-Myc-overexpressing human B-cell non-Hodgkin lymphomas. *Int J Cancer* 135:2034–2045
- Zheng H, Ying H, Yan H, Kimmelman AC, Hiller DJ, Che AJ, Perry SR, Tonon G, Chu GC, Ding Z, Stommel JM, Dunn KL, Wiedemeyer R, You MJ, Brennan C, Wang YA, Ligon KL, Wong WH, Chin L, DePinho RA (2008) p53 and Pten control neural and glioma stem/progenitor cell renewal and differentiation. *Nature* 455:1129–1133
- Zhu L, Alმაჯა J, Dadi PK, Hong H, Sakamoto W, Rossi M, Lee RJ, Vierra NC, Lu H, Cui Y, McMillin SM, Perry NA, Gurevich VV, Lee A, Kuo B, Leapman RD, Matschinsky FM, Doliba NM, Urs NM, Caron MG, Jacobson DA, Caicedo A, Wess J (2017) β -arrestin-2 is an essential regulator of pancreatic β -cell function under physiological and pathophysiological conditions. *Nat Commun* 8:14295
- Zhuang W, Li B, Long L, Chen L, Huang Q, Liang Z (2011) Induction of autophagy promotes differentiation of glioma-initiating cells and their radiosensitivity. *Int J Cancer* 129:2720–2731

Affiliations

Francesco Marampon¹ · Flavio Leoni² · Andrea Mancini³ · Ilaria Pietrantonì⁴ · Silvia Codenotti⁵ · Ferella Letizia^{3,6} · Francesca Megiorni⁷ · Giuliana Porro² · Elisabetta Galbiati² · Pietro Pozzi² · Paolo Mascagni² · Alfredo Budillon⁸ · Roberto Maggio⁴ · Vincenzo Tombolini¹ · Alessandro Fanzani⁵ · Giovanni Luca Gravina^{3,6} · Claudio Festuccia³ 

¹ Department of Radiotherapy, Policlinico Umberto I, “Sapienza” University of Rome, Rome, Italy

² Research Center, Italfarmaco SpA, Cinisello Balsamo, Milan, Italy

³ Radiobiology Laboratory, Department of Biotechnological and Applied Clinical Sciences, University of L’Aquila, Via vetoiossnc, Coppito II, L’Aquila, Italy

⁴ Laboratory of Pharmacology, Department of Biotechnological and Applied Clinical Sciences, University of L’Aquila, L’Aquila, Italy

⁵ Department of Molecular and Translational Medicine, University of Brescia, Brescia, Italy

⁶ Division of Radiation Oncology, Department of Biotechnological and Applied Clinical Sciences, University of L’Aquila, L’Aquila, Italy

⁷ Department of Experimental Medicine, “Sapienza” University of Rome, Rome, Italy

⁸ Experimental Pharmacology Unit, Istituto Nazionale Tumori-IRCCS-Fondazione G. Pascale, Naples, Italy